*J. Fluid Mech.* (2011), *vol.* 670, *pp.* 85–95. © Cambridge University Press 2011 
doi:10.1017/S0022112010005665

# Steady vortex dipoles with general profile functions

TRENTON R. ALBRECHT, ALAN R. ELCRAT† AND KENNETH G. MILLER

Department of Mathematics, Wichita State University, Wichita, KS 67260, USA

(Received 13 March 2010; revised 16 August 2010; accepted 22 October 2010; first published online 7 February 2011)

Vortex dipoles in a two-dimensional, inviscid flow are obtained by prescribing the profile function relating the vorticity to the stream function. The profile functions used are smooth, and the solutions obtained have a smooth transition from the exterior flow to the interior of the vortex. The dipoles are nearly elliptical, and this relates this work to the 'supersmooth' dipoles obtained recently by Kizner & Khvoles (*Regular Chaotic Dyn.*, vol. 9, 2004, pp. 509–518). The solutions found here are obtained by an iterative method for solving the nonlinear partial differential equation for the stream function. This iterative method is both robust and flexible. Solutions are also obtained in a $\beta$-plane, and they are shielded, as has also been found in previous work.

**Key words:** computational methods, general fluid mechanics, vortex dynamics

## 1. Introduction

Translating vortex pairs in an inviscid fluid have been studied since the time of Kelvin and continue to be useful as a model of organized vortex structures. More generally, dipolar vortices play an important role in geophysical flows because of their robustness and long lifespan (see Flierl *et al.* 1980, Flierl, Stern & Whitehead 1983 and Flierl 1987). For a two-dimensional inviscid flow to be steady the vorticity and the stream function must be functionally related (Batchelor 1967, § 7.4), and if the flow is the zero-viscosity limit of solutions of the steady Navier–Stokes equations, then the Prandtl–Batchelor theorem (Batchelor 1956) implies that the vorticity is constant in regions with closed streamlines. Flows of this type have been widely studied using methods of contour dynamics. In particular, the 'translating V-states' of Wu, Overman & Zabusky (1984) are pairs of vortices of equal magnitude and oppositely signed vorticity. Here the 'profile function' giving vorticity as a function of the stream function can be written in terms of the Heaviside function. On the other hand any profile function yields a steady solution of the Euler equations, and there are many examples of non-constant profile functions that yield interesting and useful flows. The simplest is that obtained if the profile function is linear, and this can be used to obtain the Lamb–Chaplygin vortex in which the vorticity is confined to a circular region centred at the origin. (An extensive discussion of this solution which puts it in historical context is given in Meleshko & van Heijst 1994.)

The Lamb–Chaplygin vortex has been widely used in modelling geophysical flows, but dipoles occurring in geophysical flows are often compressed in the direction of

† Email address for correspondence: elcrat@math.wichita.edu

https://doi.org/10.1017/S0022112010005665 Published online by Cambridge University Press

translation (see Trieling *et al.* 2010), and this has motivated the study of vortices confined to elliptic regions by Kizner & Khvoles (2004), Khvoles, Berson & Kizner (2005), Trieling *et al.* (2010) and Kizner & Reznik (2010). In their work elliptic vortices have been found by assuming this shape and matching free parameters in assumed forms of the solution inside and outside the vortex region. The profile function is then obtained from a scatter diagram of vorticity and stream function values. The purpose of the present paper is to turn this around: to give a profile function and determine the shape of the vortex as part of the solution. This is accomplished by using an iterative procedure, similar to that used in Elcrat *et al.* (2000) and Elcrat, Fornberg & Miller (2001, 2008), for numerically solving the nonlinear partial differential equation satisfied by the stream function.

In our previous work we found uniform vortices for steady flow past a cylindrical or spherical obstacle. For the geophysical problems being considered here there is no obstacle, so we open our discussion by using our numerical method to obtain a symmetric flow with patches of uniform vorticity in the full plane. This gives the translating V-states previously computed by Pierrehumbert (1980) and Wu *et al.* (1984). This is described in § 2, which includes a fairly complete outline of the numerical method as it is applied in the case of both constant vorticity and more general profile functions. In § 3 we describe dipoles obtained from a smooth profile function. For the resulting solutions the vorticity makes a smooth transition to zero at the vortex boundary. A significant motivation for considering such 'supersmooth' vortices is that the numerical calculations of Kizner & Khvoles (2004) and Khvoles *et al.* (2005) suggest that there is enhanced stability when the vorticity is smooth at the vortex boundary. In § 4 we use our methods to consider flows in a $\beta$-plane approximation to flows over a sphere. As in Khvoles *et al.* (2005), in order to have a smooth transition of vorticity in the $\beta$-plane, the resulting vortices must be 'shielded' in the sense that there is a counter-rotating region surrounding the main vortex core.

For the numerical examples we discuss in §§ 3 and 4 we primarily restrict our attention to profile functions given by a single power term. We obtain results that are consistent with those in Khvoles *et al.* (2005). The vortex boundaries that we compute are quite close to elliptical in shape.

Beyond the specific computational results obtained, the main purpose of this paper is to describe a numerical method which is quite general, robust and flexible in dealing with a large class of vortical problems.

## 2. Uniform vortex patches

In this section we consider steady flows in the plane which are symmetric about the $x$-axis and irrotational except for a pair of symmetric, counter-rotating patches of constant vorticity. These flows have been studied previously by various methods, including contour dynamics (e.g. Wu *et al.* 1984) and variational methods (e.g. Turkington 1983 and Eydeland & Turkington 1988). Our purpose here is to describe how the methods developed in Elcrat *et al.* (2000, 2001) for flows past a cylinder or sphere can be modified for this problem and to set the background for dealing with more general profile functions, which will be discussed in the following sections.

By symmetry we may restrict our attention to the upper half-plane. In terms of a stream function $\psi$ that vanishes on the horizontal axis of symmetry, constant-vorticity vortex patches can be obtained as solutions of

$$\Delta\psi = \omega F(\psi - \alpha), \tag{2.1}$$

https://doi.org/10.1017/S0022112010005665 Published online by Cambridge University Press

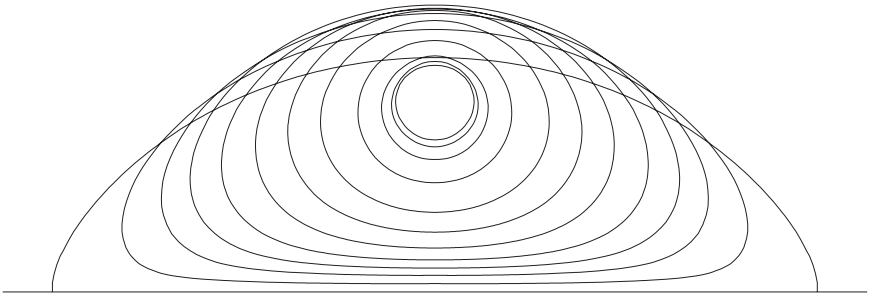


FIGURE 1. The upper half of a family of vortex pairs with fixed circulation. If the distance from the point vortex location to the axis is taken as a reference length, then the non-dimensional circulation is $\kappa/L = 4\pi$. The values of the non-dimensional quantity $-\alpha/L$ for the various solutions are 5.042, 4.098, 3.280, 2.881, 2.148, 1.432, 1.003, 0.689, 0.462, 0.315, 0.202, 0.091 and 0.

where $F = 1 - H$, with $H$ being the Heaviside function; $\omega$ is the vortex strength and $\alpha$ is the value of the stream function on the boundary of the vortex patch. The vorticity is equal to $-\omega$, $\omega > 0$, in the region in which $\psi < \alpha$. For $\alpha < 0$ the vortex region is strictly in the upper half-plane, and for $\alpha = 0$ the vortex is attached to the horizontal axis. Throughout this section $F = 1 - H$, where $H$ is the Heaviside function. Modification of the method to deal with more general $F$ will be considered in the next section.

There are solutions for all $\omega > 0$ and all $\alpha \leqslant 0$. However, note that if $L$ is a reference length, then $\hat{\psi} = \psi/L$, $\hat{\alpha} = \alpha/L$ and $\hat{\omega} = \omega L$ are the corresponding non-dimensional quantities. Two solutions with parameter values $(\alpha_1, \omega_1)$ and $(\alpha_2, \omega_2)$ are dynamically similar if $\alpha_1\omega_1 = \alpha_2\omega_2$, so there is only a one-parameter family of dynamically distinct solutions. (Here we are assuming that given $\omega > 0$ and $\alpha \leqslant 0$ the solution is unique, although this has never been proven. Some uniqueness theorems for other flows related to vortex pairs are given in Kloeden 1987 and Burton 1996.) Figure 1 shows these solutions as vortex patch desingularizations of a point vortex dipole, each desingularization having the same circulation $\kappa$ as the point vortex. Letting $A$ denote the area of the vortex patch, the circulation $\kappa$ around the patch is given by $\kappa = \omega A$. We note that rather than holding $\kappa$ fixed, in their computations Pierrehumbert (1980) and Wu *et al.* (1984) fixed the maximum distance from a point on the vortex boundary to the $x$-axis.

We now describe the algorithm that we use for computing these solutions. For this algorithm it is necessary to fix $A$, the numerical procedure being unstable if $A$ is allowed to vary without bound. We can either prescribe $\alpha$ also and determine $\omega$ as part of the solution or, alternatively, prescribe $A$ and $\omega$ and determine $\alpha$ as part of the solution. Since the primary interest in the following sections of the paper is the situation in which part of the dipole boundary is along the $x$-axis, i.e. $\alpha = 0$, we primarily use the version of the algorithm that fixes $\alpha$ in this paper. Our description of the algorithm will be for that case only; the version with $\omega$ fixed is similar. We note that our algorithm also converges for a range of $\alpha > 0$, in which case the vortex region extends to infinity in both directions along the axis of symmetry. We have no need for these solutions here, so they will not be discussed further. For a flow past a cylinder and for an axisymmetric flow with swirl, such solutions are described in Elcrat *et al.* (2000, 2008).

For a given $A$ and $\alpha$, our iterative procedure for solving the nonlinear equation (2.1) involves solving the linear equation

$$\Delta\psi_{n+1} = \omega_{n+1} F(\psi_n - \alpha) \tag{2.2}$$

https://doi.org/10.1017/S0022112010005665 Published online by Cambridge University Press

efficiently. The area of the set $\{\psi_{n+1} < \alpha\}$ depends monotonically on the value of $\omega_{n+1}$, so an inner iteration, based on the secant method, is used to determine a value of $\omega_{n+1}$ so that the area of $\{\psi_{n+1} < \alpha\}$ is equal to $A$ to within some prescribed tolerance, usually taken to be $h^2$, where $h$ is the grid spacing in the computational domain (to be described in the next paragraph). We use linear interpolation to calculate the area of $\{\psi_{n+1} < \alpha\}$, as discussed in Elcrat *et al.* (2000). Iterations are continued until the set of grid points in $\{\psi_{n+1} < \alpha\}$ is the same as the set of grid points in $\{\psi_n < \alpha\}$.

In discretizing (2.2), we first transform the upper half of the flow domain, $\mathrm{Im}(z) > 0$, to an infinite strip via the map $w = \mathrm{i}\ln(z)$. Letting $w = \xi + \mathrm{i}\eta$ and $\Psi(\xi, \eta) = \psi(x, y)$, (2.2) transforms to

$$\Delta\Psi_{n+1} = \omega_{n+1} \mathrm{e}^{2\eta} F(\Psi_n - \alpha). \tag{2.3}$$

To obtain a bounded computational domain we truncate the infinite strip to $a < \eta < b$ which corresponds to truncating the flow domain to $\mathrm{e}^a < |z| < \mathrm{e}^b$. We discretize (2.3) using the standard five-point stencil for a uniform $M \times N$ grid in this computational domain. Typically we take $b = \pi$, $N = 400$ and $a \sim \ln(0.05)$, the exact value of $a$ being restricted by the requirement that the grid rectangles should be square. The sparse matrix functionality of Matlab is used to solve the resulting $M \times N$ by $M \times N$ linear system at each step. Writing $\Phi = \Psi - \Psi_o$, where $\Psi_o = -\mathrm{e}^\eta \sin\xi$ is the stream function for potential flow in $(\xi, \eta)$ coordinates, the boundary condition for $\Phi$ on the lateral sides of the computational rectangle, which correspond to part of the horizontal axis in the physical domain, is $\Phi = 0$. As in Elcrat *et al.* (2001), to obtain a reasonable numerical boundary condition on the upper boundary, $\eta = b$, consider the series expansion of $\Phi$ in terms of the functions $\mathrm{e}^{k\eta}\sin k\xi$, $k \in \mathbb{Z}$. Uniform flow at infinity implies that no terms with $k \geqslant 0$ can occur, and it is reasonable to assume that terms with $k < -1$ can be neglected. The remaining term satisfies a Robin condition,

$$\frac{\partial\Phi}{\partial\eta} + \Phi = 0, \tag{2.4}$$

which we take as the boundary condition on the upper boundary, $\eta = b$. On the lower boundary, $\eta = a$, we can impose a Dirichlet condition based on a linear approximation $\psi(x, y) \sim cy$ for the stream function for $y$ near 0. The value of $c$, updated at each iteration, is obtained from a numerical estimate of $\partial\Phi/\partial\xi$ on the lateral side of the computational domain.

We can compare our computed solutions with the computed translating V-states given in Wu *et al.* (1984). In particular we have compared the aspect ratios of several of our solutions with the values given in table 1 of Wu *et al.* (1984), including the attached case $\alpha = 0$. The values we obtained generally differ from those in Wu *et al.* (1984) by less than $h/2$, where $h$ is the grid spacing in the parameter domain. Typically $h \approx 0.01$ in our calculations. It was also noted in our previous work with this algorithm (Elcrat *et al.* 2000, 2001) that accuracy of the order of $h$ in the location of the free boundary is expected. Since this is obtained by linear interpolation along the boundary of a grid rectangle this is as good as can be expected.

## 3. General profile functions

We consider here profile functions $F$ in which the transition from zero to non-zero values of vorticity is continuous, with particular emphasis placed on cases in which this transition is continuously differentiable. As discussed in the Introduction, there is some reason to believe that dipoles with such profile functions are less sensitive to

https://doi.org/10.1017/S0022112010005665 Published online by Cambridge University Press

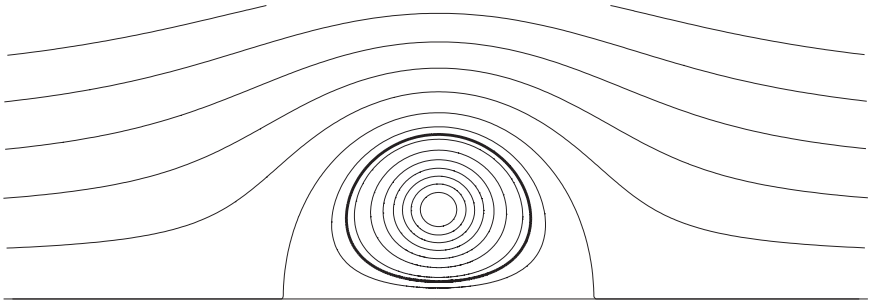


FIGURE 2. Upper half-plane streamline plot for a smooth profile dipole, $\gamma = 3$, with $\alpha < 0$. The thicker curve indicates the vortex boundary $\{\psi = \alpha\}$, the flow being irrotational outside. Taking the maximum distance from a point on the vortex boundary to the horizontal axis as a reference length, the dimensionless $\alpha$ for the plot shown is $-0.315$. The corresponding vortex patch, with a Heaviside profile (see figure 1), is more elongated in the horizontal direction.

instabilities and more likely to correspond to what is observed in nature (see Khvoles *et al.* 2005 and Trieling *et al.* 2010 and the references therein). To fix ideas we set

$$F(\psi) = H(-\psi)(-\psi)^{\gamma}, \ \gamma \geqslant 1, \tag{3.1}$$

and we solve

$$\triangle\psi = \omega F(\psi - \alpha), \tag{3.2}$$

with $\omega = \omega(A)$ adjusted as in the previous section to achieve a given area. The parameter $\omega$ is now related to the circulation $\kappa$ by

$$\kappa = \omega \int_D (-\psi)^{\gamma}, \tag{3.3}$$

where $D = \{\psi < \alpha\}$.

The algorithm described in the previous section is used with the following modification: the procedure terminates when the $L^1$ norm of the difference between iterations satisfies some prescribed (relative) convergence criterion, usually taken to be 1 % in the computations described below.

If $\gamma > k$, then the vorticity is $k$ times continuously differentiable at $\psi = \alpha$, and we might designate these vortices as 'supersmooth' if $\gamma > 1$, as in Kizner & Khvoles (2004). We have chosen profile functions of the form (3.1) on the basis of their simplicity and also because of the shapes of the computed profile functions in Kizner & Khvoles (2004). The $\alpha = 0$ case yields dipoles comparable to those considered in Kizner & Khvoles (2004) and Khvoles *et al.* (2005), and the solutions can then be called 'supersmooth dipoles'. For completeness we give one solution with $\alpha < 0$ (see figure 2) but restrict our attention to $\alpha = 0$ for the remainder of the paper.

In Kizner & Khvoles (2004) an elliptical vortex shape was imposed, and solutions were obtained by matching analytical formulae at the boundary. Here we impose a profile function and get the vortex boundary as part of the solution. All of the vortices obtained in the range $\gamma \geqslant 1$ are close to elliptical. To measure this closeness we compute the least-squares deviation of the vortex boundary from an ellipse whose aspect ratio is that of the computed vortex boundary, relative to the distance from the origin. For $\gamma = 1$ this least-squares deviation from an ellipse decreases linearly with grid size and appears to approach 0, as expected, since the $\gamma = 1$ solution is the Lamb–Chaplygin vortex which has a circular boundary. For $\gamma \geqslant 2$ the relative least-squares deviation from an ellipse also decreases with decreasing grid size but

https://doi.org/10.1017/S0022112010005665 Published online by Cambridge University Press

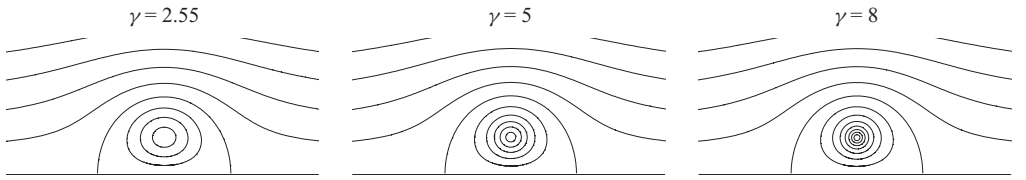



FIGURE 3. Streamline plots for three different values of $\gamma$, with $\alpha = 0$. The separatrix is nearly elliptical in each case; the aspect ratio increases from 1.16 when $\gamma = 2.55$ to 1.21 when $\gamma = 8$. The aspect ratio of the solutions we obtain most closely matches that of the supersmooth elliptic dipole found by Kizner & Khvoles (2004) when $\gamma = 2.55$. In the plots in this figure the spacing between contour levels is constant and the same in each subplot. Flow speeds are greater near the centre when $\gamma$ is larger. Also the total circulation inside the upper half of the dipole increases with $\gamma$: the circulation for $\gamma = 8$ is about 12 % larger than for $\gamma = 2.55$.

stabilizes at a value in the 0.2–0.3 % range. This deviation is barely visible in typical plots; however it is more than 10 times the smallest deviation obtained for the Lamb–Chaplygin vortex. There is no analytical reason to expect that solutions obtained using the profile function (3.1) should yield exactly elliptical vortex regions. As $\gamma$ varies from 1 to 0 the vortex boundary becomes visibly less elliptical and approaches the $\alpha = 0$ uniform vortex patch discussed in the previous section.

As the power $\gamma$ increases, the aspect ratio $b/a$ of the computed vortex increases monotonically. (Here $a$ and $b$ are the positive $x$ and $y$ intercepts on the vortex boundary.) Our calculations suggest that there is an upper bound of about 1.21 for this aspect ratio, although calculations with $\gamma$ much larger than 10 are not very accurate. As can be seen in figure 3, as $\gamma$ increases, flow speeds near the centre increase. The circulation $\kappa$ also increases as $\gamma$ increases.

All of these vortex dipoles with $\gamma > 1$ are supersmooth in the sense that the first derivative of the vorticity is continuous at the interface between the vortex and the surrounding irrotational flow. Our results do not contradict the claim made in Kizner & Khvoles (2004) that only one elliptic dipole is supersmooth, since the dipoles we have computed, although close to elliptical, are probably not exact ellipses. Our solution with $\gamma = 2.55$ yields an aspect ratio of 1.162, the aspect ratio of the supersmooth elliptic dipole found in Kizner & Khvoles (2004).

In the above results, we obtained vortices elongated in the vertical direction, i.e. with the aspect ratio >1. In the earlier work of Boyd & Ma (1990) an elliptical shape elongated in the horizontal direction was imposed. We have used their results to guess a form for an appropriate profile function and used our methods to compute the solutions. The results were in qualitative agreement with Boyd & Ma (1990). In particular with profile function $F(-\psi)H(-\psi)$, where $F(\psi) = \omega a \psi \mathrm{e}^{-a\psi}$, the vortices became more hollow as $a$ increased; that is, the vorticity was more concentrated near the boundary of the vortex, and the nearly elliptical shapes became thinner as in Boyd & Ma (1990).

## 4. Solutions in a $\beta$-plane

If the dipole translates in a layer of fluid above a rotating sphere and the $\beta$-plane approximation is invoked, i.e. the first term in the Taylor series expansion of the Coriolis term is kept, we obtain

$$J(\psi, q) = 0, \tag{4.1}$$

https://doi.org/10.1017/S0022112010005665 Published online by Cambridge University Press

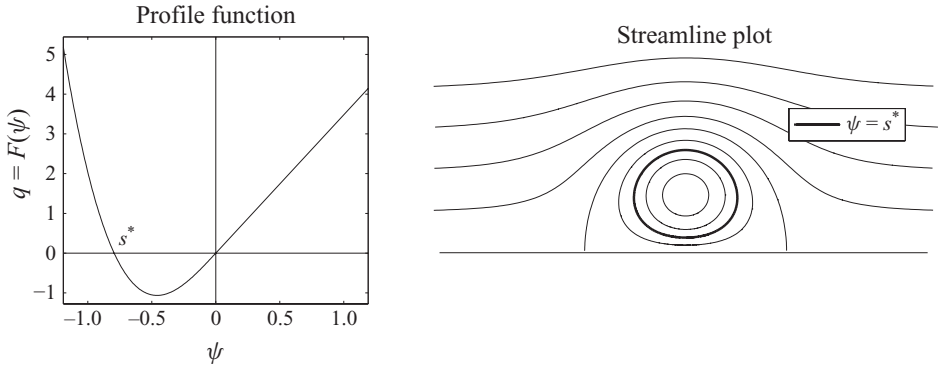



FIGURE 4. Typical profile function and streamline plot, $\beta > 0$. In the 'shield', i.e. the region $\{(x, y)\colon s^* < \psi(x, y) < 0\}$, $s^* = -(\beta/\lambda)^{(1/(\gamma-1))}$, the potential vorticity $q$ is negative. In the inner core, $\{(x, y)\colon \psi(x, y) < s^*\}$, $q$ is positive. For the flow shown, $\gamma = 3$. Dimensionless values of $\beta$ and $s^*$ are 3.48 and $-0.794$ respectively, where the reference length is taken to be the maximum distance from a point on the vortex boundary to the horizontal axis.

where $q$ is the potential vorticity, $q = \triangle\psi + \beta y$, in which $\beta$ is the Coriolis parameter (see Flierl *et al.* 1980; Khvoles *et al.* 2005). This implies the following equation:

$$\triangle\psi + \beta y = F(\psi). \tag{4.2}$$

Note that the streamlines $\psi = c$, $c > 0$, extend to infinity, and uniform velocity at $\infty$ implies that $\psi(x, y) \to y$ as $x \to \infty$ along such a streamline. Also $\Delta\psi \to 0$ as $x \to \infty$ along such a streamline, so (4.2) implies $F(\psi) = \beta\psi$ for $\psi > 0$. In order to have (two) continuous derivatives at the vortex boundary $\psi = 0$, we assume that

$$F(\psi) = \begin{cases} \beta\psi + \lambda(-\psi)^\gamma & \text{for } \psi < 0, \\ \beta\psi & \text{for } \psi > 0, \end{cases} \tag{4.3}$$

with $\gamma > 2$. The inclusion of the term $\beta\psi$ in the profile function for the interior of the vortex, required for smoothness, also requires that the core is 'shielded'; i.e. there is a band of oppositely signed vorticity surrounding the core, as discussed in Khvoles *et al.* (2005) (see figure 4). The parameter $\lambda$ in (4.3) plays the algorithmic role that $\omega$ did when $\beta = 0$.

We remark here that if dimensionless variables are introduced the equations have exactly the same form. We may then assume that the solutions presented are given in dimensionless variables if it is convenient, and this has been done in figures 4 and 5. Dimensionless values for $\beta$ can be given in dimensional variables by $\beta L^2/U$, where $L$ is a reference length and $U$ is the velocity at infinity. If $L$ is fixed (or varies only slightly as in figure 5) we may think of large $\beta$ as being equivalent to small $U$. In Flierl (1987) a $\beta$-plane point vortex model is discussed in which, for one branch of solutions, $U$ goes to zero with increasing circulation. The details of the flow are different, but the analogy is suggestive.

We have computed a sequence of solutions for increasing values of $\beta$ with $\gamma = 3$. The convergence slowed considerably at the largest value of $\beta$ shown in figure 5, and the solutions appear to be approaching a singular behaviour. The area of the central region, where the potential vorticity is positive, decreases, while the the magnitude of the values for $\psi$ increase with increasing $\beta$, and the value of the equilibrium value of $\lambda$ decreases. The circulations in both the central region and the 'shield' increase in absolute value dramatically more than the total circulation increases.

https://doi.org/10.1017/S0022112010005665 Published online by Cambridge University Press

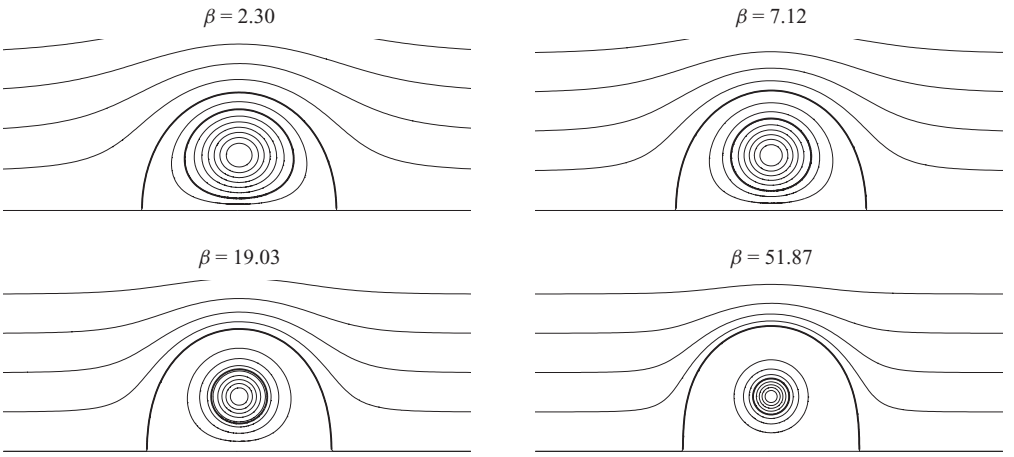



FIGURE 5. Solutions for non-dimensional values of $\beta$, where the reference length is taken to be the maximum distance from a point on the vortex boundary to the horizontal axis. In each case, $\gamma = 3$. Non-dimensional values of the total vortex circulation in the region $\{\psi < 0\}$ for the four examples, with increasing $\beta$, are 11.35, 18.22, 32.77 and 75.45, while the inner-core circulations are 11.57, 20.38, 50.78 and 286.6, respectively.

We have also computed a set of solutions with increasing $\beta$ in order to compare with the supersmooth shielded vortices described in Khvoles *et al.* (2005, p. 9, figure 1). As shown in figure 6, for non-dimensional $\gamma = 2.55$, the aspect ratios of our solutions and theirs are close for small $\beta$, but for larger $\beta$ the elliptical solutions of Khvoles *et al.* (2005) and our solutions differ. For completeness we have included solutions for several other values of $\gamma$. All of these solutions are smooth in the sense that derivatives of the profile function are continuous at the vortex boundary. For each $\gamma$, as $\beta$ increases, the vortex boundaries become less elliptical. Using the measure described in § 3, the mean relative deviation from an ellipse for the vortex with the largest value of $\beta$ shown in figure 5 is about 2 %.

## 5. Discussion and conclusions

We have described a method for computing vortex dipoles by using an iterative procedure for solving the nonlinear Poisson equation for the stream function. In the recent work by Kizner & Khvoles (2004) and Khvoles *et al.* (2005) on geophysical flows, elliptic dipoles were found using a matching procedure at the ellipse boundary, with the profile function then determined numerically from a scatter plot of vorticity and stream function values. Our procedure turns this approach around: the profile function is prescribed at the outset, and the shape of the vortex region is determined from the solution. Our results are quite consistent with the results obtained by Kizner & Khvoles (2004) and Khvoles *et al.* (2005) but do not duplicate those results. The profile functions they compute are not necessarily of the form we prescribe (although they indicate that the linear and cubic terms dominate when the profile function is expanded in odd powers). Likewise, the vortex regions we have obtained are close to elliptical but not necessarily exact ellipses, as discussed in § 3.

Other authors have also used prescribed profile functions. In particular Eydeland & Turkington (1988) have considered convex profile functions with polynomial growth by using variational methods. They have obtained solutions by maximizing the energy

https://doi.org/10.1017/S0022112010005665 Published online by Cambridge University Press

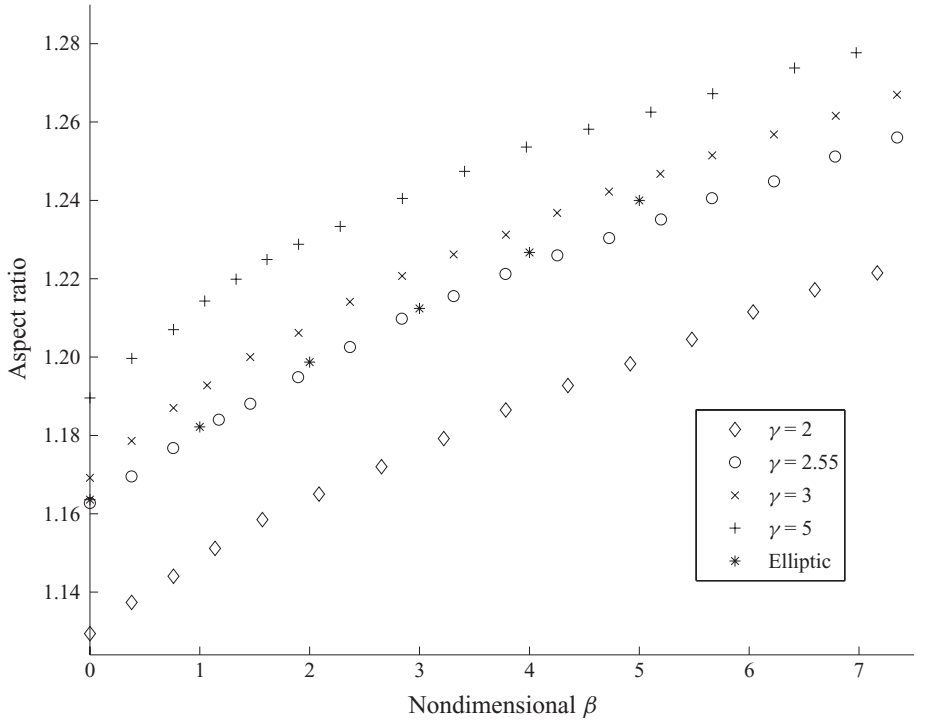



FIGURE 6. Aspect ratio versus $\beta$ for four values of the exponent $\gamma$. The elliptic data are for supersmooth elliptic modons, taken from figure 1 of Khvoles *et al.* (2005).

subject to a circulation constraint. Vortex patches are a limiting case, and then the vorticity $\omega$ is fixed, and the constraint is equivalent to fixing the area. The value of the stream function on the vortex boundary is a Lagrange multiplier for this constraint. In our algorithm we have fixed the value of the stream function on the boundary, and the value of $\omega$ was found as a part of the solution. We may think formally of $\omega$ as a Lagrange multiplier for maximizing the energy subject to an area constraint, but we have made no attempt to give this idea a rigorous formulation here. In a related work Burton (1989) has found profile functions theoretically by using the methods of functional analysis from solutions of variational problems. He used the Kelvin–Benjamin variational principle (see Benjamin 1976) in which energy is maximized over functions which are rearrangements of a fixed function. The intuitive interpretation of this constraint is that the measures of the sets in which the vorticity is less than $c$ are prescribed for all $c$. This is motivated by the fact that the time-evolved vorticity in two-dimensional flow is related to the initial vorticity in this way.

Elcrat & Miller (1995) have given sufficient conditions for solutions obtained from these variational problems to provide desingularizations of equilibrium states of point vortices. This leads naturally to the question of how to conduct a search of the large parameter space for steady vortex solutions. For travelling V-states the translating point vortex pair is the natural reference flow in organizing parameters, as discussed in § 2. For flows past a circular cylinder and the solutions found in Elcrat *et al.* (2000) the possible point vortex solutions played a similar role. The idea there was to grow finite-area vortices from point vortices by increasing the area with the circulation fixed. We believe that this is a natural strategy in general.

https://doi.org/10.1017/S0022112010005665 Published online by Cambridge University Press

For general profiles we may think of patches or explicit solutions such as that of Lamb and Chaplygin as a guide for what may be possible and for appropriate initial guesses in our algorithm. In this work we have simply chosen profile functions which are qualitatively similar to those found in Kizner & Khvoles (2004) and Khvoles *et al.* (2005). In other contexts they might be chosen on the bases of physical principles or experimental observations. In a study of possible models for atmospheric blocking Verkley (1993) has found flows with nonlinear relations between stream functions and vorticity in a flow over a sphere. These relations were found from scatter diagrams which were in turn obtained from computations based on atmospheric data.

The computational algorithm that we have used is very robust. Although it is based on the simple idea of successive iteration, it converges even for very crude initial guesses. This is quite likely due to the smoothing properties of the linear elliptic operators involved. In particular, if the initial guess for the vortex support on the right-hand side of (2.2) is highly disconnected, e.g. if $\alpha - \psi_0$ is the characteristic function of a randomly chosen set of grid points, then after one iteration the vortex support $\{\psi_1 < \alpha\}$ is connected.

An important question concerns the stability of these solutions. In Elcrat, Fornberg & Miller (2005) we studied stability for uniform vortex patch desingularizations of Föppl point vortices, using methods related to contour dynamics. For the non-uniform vortices, which have been the primary concern here, different methods are required, and we plan to return to this question in subsequent work. It should also be pointed out that the primary motivation for introducing non-circular dipoles has been to find vortices with a smooth transition to irrotational flow because it is believed that this would enhance stability. In several works (e.g. Kizner & Khvoles 2004 and Khvoles *et al.* 2005), time-dependent computations for the Euler equations have supported this. Vortex dipoles with a profile with a cubic nonlinearity have previously been studied by Hesthaven *et al.* (1995). They found shielded vortices and studied the stability of these structures as well as interaction with other dipoles. More recently Kizner, Khvoles & Kessler (2010) have shown that if viscous effects are included, then a specific nearly elliptical, quasi-asymptotic limiting state is selected as viscosity goes to zero.

One useful feature of the methods that we have used here is their flexibility. It is routine, for example, to change the nature of the profile function or to modify the external flow, and the procedure we have used is not dependent on analytical solution forms that arise from explicit solutions.

## REFERENCES

Batchelor, G. K. 1956 On steady laminar flow with closed streamlines at large Reynolds number. *J. Fluid Mech.* **1**, 177–190.

Batchelor, G. K. 1967 *An Introduction to Fluid Dynamics.* Cambridge University Press.

Benjamin, T. B. 1976 The alliance of practical and analytical insights into the non-linear problems of fluid mechanics. In *Applications of Methods of Functional Analysis to Problems in Mechanics* (ed. P. Germain & B. Neyroles), Lecture Notes in Mathematics, vol. 503, pp. 8–29. Springer.

Boyd, J. & Ma, H. 1990 Numerical study of elliptical modons using spectral methods. *J. Fluid Mech.* **221**, 597–611.

Burton, G. R. 1989 Rearrangements of functions, saddle points and uncountable families of steady configurations for a vortex. *Acta Math.* **163**, 291–309.

Burton, G. R. 1996 Uniqueness for the circular vortex-pair in a uniform flow. *Proc. R. Soc. Lond.* A **452**, 2343–2350.

Elcrat, A. R., Fornberg, B., Horn, M. & Miller, K. 2000 Some steady vortex flows past a circular cylinder. *J. Fluid Mech.* **409**, 13–27.

https://doi.org/10.1017/S0022112010005665 Published online by Cambridge University Press

Elcrat, A. R., Fornberg, B. & Miller, K. 2001 Some steady axisymmetric vortex flows past a sphere. *J. Fluid Mech.* **433**, 315–328.

Elcrat, A. R., Fornberg, B. & Miller, K. G. 2005 Stability of vortices in equilibrium with a cylinder. *J. Fluid Mech.* **544**, 53–68.

Elcrat, A. R., Fornberg, B. & Miller, K. G. 2008 Steady axisymmetric vortex flows with swirl and shear. *J. Fluid Mech.* **613**, 395–410.

Elcrat, A. R. & Miller, K. 1995 Rearrangements in steady multiple vortex flows. *Commun. Part. Differ. Equ.* **20**, 1481–1490.

Eydeland, A. & Turkington, B. 1988 A computational method of solving free-boundary problems in vortex dynamics. *J Comput. Phys.* **78**, 194–214.

Flierl, G. 1987 Isolated eddy models in geophysics. *Annu. Rev. Fluid Mech.* **19**, 493–530.

Flierl, G., Larichev, V., McWilliams, J. & Reznik, G. 1980 The dynamics of baroclinic and barotropic solitary eddies. *Dyn. Atmos. Oceans* **5**, 1–41.

Flierl, G., Stern, M. & Whitehead, J. Jr. 1983 The physical significance of modons: laboratory experiments and integral constraints. *Dyn. Atmos. Oceans* **7**, 233–263.

Hesthaven, J. S., Lynov, A. H., Nielsen, A. H., Rasmussen, J. J. & Schmidt, M. R. 1995 Dynamics of a nonlinear dipole vortex. *Phys. Fluids* **7**, 2220–2229.

Khvoles, R., Berson, D. & Kizner, Z. 2005 The structure and evolution of elliptical barotropic modons. *J. Fluid Mech.* **530**, 1–30.

Khvoles, R., Kizner, Z. & Kessler, D. 2010 Viscous selection of an elliptical dipole. *J. Fluid Mech.* **658**, 492–508.

Kizner, Z. & Khvoles, R. 2004 Two variations on the theme of Lamb–Chaplygin: supersmooth dipole and rotating multipoles. *Regular Chaotic Dyn.* **9**, 509–518.

Kizner, Z. & Reznik, G. 2010 Localized dipoles: from 2D to rotating shallow water. *Theor. Comput. Fluid Dyn.* **24**, 101–110.

Kloeden, P. 1987 On the uniqueness of solitary Rossby waves. *J. Austral. Maths Soc.* B **28**, 476–485.

Meleshko, V. & van Heijst, G. 1994 On Chaplygin's investigations of two-dimensional vortex structures in an inviscid fluid. *J. Fluid Mech.* **272**, 157–182.

Pierrehumbert, R. 1980 A family of steady, translating vortex pairs with distributed vorticity. *J. Fluid Mech.* **99**, 129–144.

Trieling, R., Sandbergen, R., van Heijst, G. & Kizner, Z. 2010 Barotropic elliptical dipoles in a rotating fluid. *Theor. Comput. Fluid Dyn.* **24**, 111–115.

Turkington, B. 1983 On steady vortex flows in two dimensions. Part II. *Commun. Part. Differ. Equ.* **8**, 1031–1071.

Verkley, W. T. M. 1993 A numerical method for finding form-preserving free solutions of the barotropic vorticity equations on a sphere. *J. Atmos. Sci.* **50**, 1488–1503.

Wu, H. M., Overman, E. A. II & Zabusky, N. J. 1984 Steady-state solutions of the Euler equations in two dimensions: rotating and translating V-states with limiting cases. Part I. Numerical algorithms and results. *J. Comput. Phys.* **53**, 42–71.

https://doi.org/10.1017/S0022112010005665 Published online by Cambridge University Press